Application of LuTan-1 SAR Data in Railway Subsidence Monitoring

Wenhao Li [1, 2], Tao Li [2], Xiaoqing Zhou [2], Xian Liu [1]

[1] Space Engineering University, Beijing, China, 101416-2583107574@qq.com
[2] Land Satellite Remote Sensing Application Center, Ministry of Natural Resources of P.R. Beijing, China, 100048-zhouxq@lasac.cn

Keywords: LuTan-1, SAR, Railway Corridor, Subsidence Monitoring.

Abstract

InSAR technology is currently a crucial tool for large-scale surface deformation monitoring, particularly excelling in regional subsidence monitoring. In this study, focusing on the Jinan section of the Shandong railway, newly launched LUTAN-1 satellite SAR data was employed. DInSAR and Stacking techniques were applied to analyze the subsidence in response to the long-term operation load of high-speed trains and surrounding human activities. Through the analysis of data from June 2023 to December 2023, regional subsidence was identified in this section, with a subsidence rate reaching 8 cm/year. Comparative analysis between DInSAR technology monitoring results and precise leveling monitoring results showed consistency in the subsidence deformation trend in the region, achieving centimeter-level deformation monitoring in the study area.The LuTan-1 satellite provided robust SAR data support for railway subsidence monitoring, offering substantial reliability and accuracy to deepen the understanding of railway subsidence issues. These research findings hold significant practical implications for adopting timely maintenance and repair measures, ensuring the safety and reliable operation of the railway system.

1. Background

1.1 Introduction

The L-band Differential Interferometric Synthetic Aperture Radar (DInSAR) satellite, also known as "LuTan-1," is China's first civil L-band SAR satellite primarily designed for terrain mapping and deformation monitoring. The LUTAN-1 constellation supports two different flight formations, as illustrated in Figure 1. The first is a dual-satellite formation used for topographic mapping and corresponding data collection. The second mode is a tandem flight mode, where the satellites follow each other to maintain a phase difference of 180°, providing single-satellite observational data for deformation monitoring.LUTAN-1 exhibits excellent performance in deformation monitoring, owing to its longer wavelength, which imparts robust penetration capability and good penetration through vegetation and cloud cover, making it suitable for areas with dense vegetation. The twin LUTAN-1 satellites operate on the same orbital plane, allowing for a differential interferometric observation with 3m high-resolution image data of the same area within a 4-day interval, ensuring high consistency in the acquired data. Therefore, utilizing InSAR technology enables the monitoring of ground deformation with centimeter to even millimeter precision(High, W., 2020).
These two satellites were successfully launched on January 26, 2022, and February 28, 2022, at the Jiuquan Satellite Launch Center. The SAR sensor is equipped with six different imaging modes featuring various spatial resolutions and imaging widths, with the key parameters outlined in Table 1. LuTan-1 has demonstrated its versatility in multiple applications. Starting from April 2023, the LuTan-1 satellite will consistently provide high-quality observational data, offering support for global natural resource monitoring, particularly in disaster monitoring and early warning applications(Gao, W., Gan, J., & Wang, C, 2015).

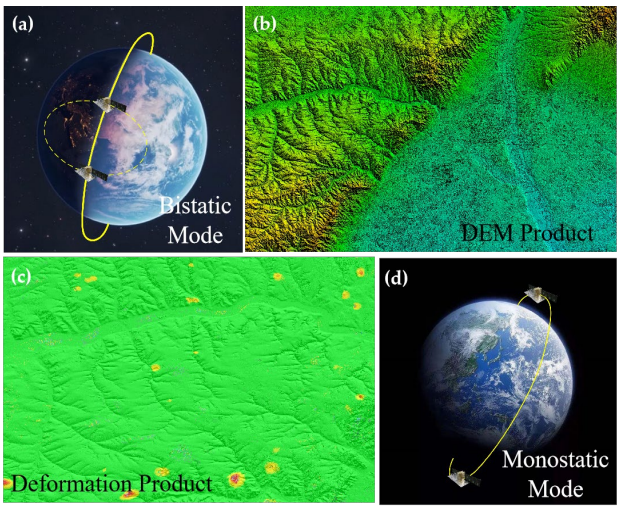

Figure 1. Satellite constellation art view and related products

Railways, as the backbone of the comprehensive transportation system, are a pioneering field for accelerating the construction of a strong transportation nation and an important support for the construction of Chinese-style modernization. By 2025, China National Railway Group Co., Ltd. (hereinafter referred to as: China Railway) will have basically completed the "six modern systems" and achieved the goals of the railway's "14th Five-Year" development plan. As China's railway, especially high-speed railway, continues to increase its operational mileage, improving the safety environment along the railway becomes more prominent in ensuring high-quality railway

development and the safety of people's lives and property. On the one hand, the stability of the railway subgrade is affected by environmental factors such as the geological structure along the line and regional surface subsidence; on the other hand, the deformation and damage of the track slab caused by the combined effects of internal factors such as subgrade static load and train dynamic load also pose a great threat to the stability of the subgrade.

Number of Satellites		2 satellites
Satellite Weight		About 3250 kg
Designed Service Life		8 years
Center Frequency		1.26GHz
Orbit	Category	Quasi-Sun-Synchronous Near-Circular Orbit
	Height	About 607km
	Tilt Angle	97.808°
	Revolutionary Cycle	Single-satellite 8 days, dual-satellite 4 days
	Monitoring Region	From 85° South to 85° North latitude
	Descending Node Local Time	6:00 am ± 15min
	Regenerative Pipeline Control Radius	Less than 350 m
Imaging-Mode Resolution@ Swath Width @ Polarization Mode	Stripmap 1	3m@50km@ Single Polarization (HH/VV)
	Stripmap 2	12m@100km@ Single Polarization (HH/VV)
	Stripmap 3	3m@50km@ Dual Polarization (HH+HV/VV+VH)
	Stripmap 4	6m@30km@ Full Polarization (HH+HV+VH+VV)
	Stripmap 5 (Wide Coverage Test Mode)	20-30m@150-250km@ Single Polarization (HH/VV)
	Scanning Mode	30m@400km@ Single Polarization (HH/VV)

Table 1. Main Parameters of LuTan-1 Satellite

1.2 Technical Advantages

At present, the technical means for ensuring railway line safety are highly reliable. However, due to the large spatial scale of high-speed railways and the complex terrain and geological conditions in which they are located, traditional deformation monitoring methods often have limitations in terms of operational efficiency, monitoring frequency, and spatial resolution. The means of ensuring safety in the railway's external environment still rely mainly on manual inspections. The complex and changeable external environment of the railway makes it impossible for on-site personnel to fully cover inspections, making it difficult to visually detect geological disaster risks in the early stages. There are many areas around the railway safety protection zone that are inaccessible or have obstructed views, and new changes in the external environment are not discovered in a timely manner, leading to occasional safety accidents or incidents. Railway safety and smooth operation are crucial to the overall economic and social development. The Party Central Committee, the State Council, and China Railway have adopted many governance policies and measures from the perspective of management mechanism innovation, and have achieved significant results. China Railway has also promoted experimental research and the application of results in technologies such as integrated sky-earth, tower video, fiber optic, and drones, but they are all subject to various limitations and have not been popularized and implemented nationwide in a normalized and engineering manner. There is an urgent need for more universal, advanced, and efficient technologies and methods to enrich and improve the means of ensuring safety in the railway's external environment and to enhance the level of informatization.

Satellite remote sensing monitoring has the characteristics of wide monitoring range, periodicity, low cost, and rapid technological updates. Satellite remote sensing monitoring data has obvious advantages as the underlying data support for the informatization of railway external environment safety. The development and application of InSAR technology has provided an important technical method for high-speed railway deformation monitoring. Based on L-band differential interferometric SAR satellites, macroscopic inspection of geological disaster risks along the railway can be carried out, paving the way for the normalized application of satellite remote sensing technology in railway external environment safety monitoring. Its high resolution and feature of continuous spatial coverage are not present in geodetic methods such as Global Positioning System (GNSS), Satellite Laser Ranging (SLR), and Very Long Baseline Interferometry (VLBI). The advantages of InSAR technology over traditional surveying techniques are shown in Table 2.

Monitoring Method	GNSS Surveying	Precise Surveying	InSAR Technology
Deformation Component	Horizontal/ Vertical	Vertical	Horizontal/ Vertical
Accuracy	5~20 mm	1~10 mm	5 mm
Sample Acquisition Frequency (1/d)	10~30	1~10	$\geqslant 10^{-6}$
Sample Density	10~100	10~100	10^{5}~100^{7}
Measurement Method	Network	Line	Surface
Monitoring Area	Small Area	Small Area	Large Area

Table 2. Comparison of InSAR Technology with Traditional Geodetic Surveying Techniques

Therefore, this study conducted a preliminary assessment of SAR data for deformation monitoring along the railway section in Jinan, Shandong. DInSAR (Li, H, 2015).technology was employed to calculate the deformation magnitude along the railway(Zhang, T., Shi, Y., Wang, J., et al, 2021). The deformation characteristics of the ground surface in the railway and surrounding areas were extracted and analyzed.

2. Methodologies And Processing Strategy

2.1 DInSAR Method

DInSAR is an extension of InSAR technology. It involves the repeated observation of the Earth's surface undergoing deformation using spaceborne SAR systems. By differencing the interferometric phase and topographic phase of SAR images before and after deformation, DInSAR eliminates terrain-induced phase and flat Earth phase, as well as mitigates atmospheric delay and noise phases, A simple schematic diagram of the radar differential interference process is shown in Figure 2. This process yields the surface deformation phase in the radar line of sight (LOS), providing information about ground deformation. DInSAR technology is particularly sensitive to vertical deformation and can achieve long-term monitoring of centimeter-level or even millimeter-level deformations over large areas. Its high resolution and continuous spatial coverage distinguish it from other geodetic measurement methods such as Global Positioning System (GPS), Satellite Laser Ranging (SLR), and Very Long Baseline Interferometry (VLBI).

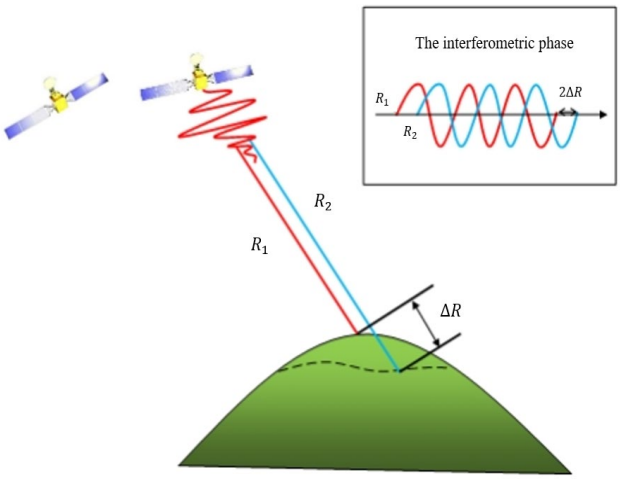

Figure 2 A simple schematic diagram of the radar differential interferometry process. In this diagram, R1 represents the slant range corresponding to the satellite's first pass, R2 represents the slant range corresponding to the satellite's second pass, and the difference between the two slant ranges (ΔR) represents the deformation parameter that InSAR aims to obtain.

The interferometric phase of SAR images before and after deformation in the same area can be represented by the following formula:

$$\phi_{wrp} = \phi_{def} + \phi_{flat} + \phi_{atmo} + \phi_{orb} + \phi_{topo} + \phi_{noise} + 2k\pi \quad (1)$$

In the formula, where ϕ_{def} 、 ϕ_{flat} 、 ϕ_{atmo} 、 ϕ_{orb} 、 ϕ_{topo} and ϕ_{noise} respectively represent the deformation phase, flat Earth phase, atmospheric phase, orbit error phase, topographic phase, and decoherence/thermal noise phase. Using precise satellite orbit data and baseline information from interferometric pairs, the orbit error phase and flat Earth phase are removed. External DEM data is used to eliminate the topographic phase. The influence of decoherence/thermal noise phase can be mitigated through filtering. For the sake of simplicity in understanding and calculation, the impact of atmospheric delay phase is ignored here. Therefore, the deformation phase can be expressed as:

$$\phi_{def} = \phi_{wrp} - \phi_{flat} - \phi_{topo} \quad (2)$$

In accordance with the principles of the InSAR method, it can be derived that:

$$\phi_{wrp} = -\frac{4\pi\left(R_1 + \Delta r - R_2\right)}{\lambda} = -\frac{4\pi\left(R_1 - R_2\right)}{\lambda} - \frac{4\pi\Delta r}{\lambda} \quad (3)$$

Therefore, the deformation phase at the ground point is:

$$\phi_{def} = -\frac{4\pi\Delta r}{\lambda} \quad (4)$$

Finally, through transformation, the deformation change along the radar line of sight for the ground object can be determined Δr .

2.2 Stacking InSAR Method

Railway subsidence along the ground is a gradual process that typically requires long-term monitoring to fully understand surface changes. Time series InSAR technology, with its advantages of high spatiotemporal resolution, long-term monitoring, real-time monitoring, and sensitivity to periodic changes, makes it an ideal choice for railway subsidence monitoring. This method can provide railway managers with timely, accurate, and comprehensive surface deformation information, helping to prevent and promptly address railway subsidence issues and improve the safety and reliability of the railway system.

Commonly used methods include Stacking technology, Wavelet time series InSAR, Small Baseline Subset (SBAS) method, Permanent Scatterers (PS), and Distributed Scatterers (DS) algorithms. These methods provide high spatiotemporal resolution surface deformation information by integrating SAR observations from multiple times, effectively suppressing the effects of temporal and spatial decorrelation, DEM residuals, and atmospheric disturbances. They greatly compensate for the shortcomings of traditional differential interferometry and can obtain high-precision (from millimeter to sub-millimeter level) surface deformation rates and sequences more accurately.

Time series SAR analysis offers long-term dynamic monitoring of surface subsidence along railways, identifying seasonal, periodic, and gradual subsidence characteristics, and provides high-precision subsidence rates and cumulative amounts. Time series SAR analysis helps to understand the cumulative effects and trends of subsidence, providing support for regional situation analysis.

The Stacking InSAR technology used in this article, also known as Interferogram Stacking, is a relatively efficient and straightforward deformation detection technique. In contrast to DInSAR technology, Stacking InSAR can significantly mitigate atmospheric effects without relying on external data, and it can suppress the impact of DEM (Digital Elevation Model) errors, thereby extracting more accurate information about surface deformation. It involves weighted averaging of unwrapped phases obtained over a certain period to weaken the influence of unrelated noise, including factors such as atmospheric effects. In traditional dual-orbit differential InSAR data processing, under specific spatiotemporal baseline constraints, high-quality

interferometric phase maps are selected to extract phase information of surface deformation at multiple time points.

The phases from multiple consecutive interferometric pairs are then superimposed to obtain the cumulative amount of surface deformation over the entire observation period. The main reason Stacking technology reduces atmospheric influence is the assumption that the presence of the atmosphere can be treated as a random signal changing over time, meaning the delay phases corresponding to each interferogram are uncorrelated. When averaging unwrapped phases over multiple consecutive times, random errors like atmospheric effects are significantly attenuated.

Before performing the stacking solution on interferograms, it is necessary to transform the acquired SAR data into a common coordinate space. Then, a least squares processing is employed to calculate the deformation information corresponding to each moment in time. The mathematical model for the Stacking technology solution is defined as follows:

$$\bar{V} = \sum_{i=1}^{N} d_i \bullet \Delta T_i / \sum_{i=1}^{N} d_i \bullet \Delta T_i^2 \tag{5}$$

$$\sigma^2(\bar{V}) = \sum_{i=1}^{N} (d_i - \bar{V}\Delta T_i)^2 / \Delta T_i \tag{6}$$

$$std(\bar{V}) = \sum_{i=1}^{n} (d_i - \bar{V}\Delta T_i)^2 / \Delta T^2 \tag{7}$$

$$d_i = -\frac{\lambda}{4\pi}\phi_{def} \tag{8}$$

$\bar{V}$ represents the Line of Sight (LOS) average deformation rate, ϕ_{def} is the deformation phase, d_i is the deformation quantity for the i-th differential interferogram, ΔT_i is the time interval for the i-th interferogram, N denotes the number of differential interferograms involved in the solution, and $\sigma(\bar{V})$ is the standard deviation of the average deformation rate.

2.3 Processing Strategy

In the handling of railway and surrounding ground subsidence, DInSAR can provide monitoring with high sensitivity and high spatiotemporal resolution. Organize and analyze the elevation reference data in the experimental area, filter SAR images covering the railway along the monitoring requirements, and conduct DInSAR processing on the experimental images. In the treatment of railway subsidence, DInSAR can provide high sensitivity and high spatiotemporal resolution monitoring. The key processing steps of DInSAR include image registration and resampling, interferogram generation, removal of flat Earth and topographic phase, interferogram filtering and quality assessment(Wang, Z., Xu, S., Wang, N., et al, 2018), and phase unwrapping, among others(Ji, Z., Bo, H., Wang, D., et al, 2019). The final result is the differential interferometric phase dominated by surface deformation, which is used to monitor the settlement conditions along railway lines and provides high-precision information on trends and cumulative settlement amounts. It is more sensitive to deformation in the vertical direction and is capable of long-term, large-scale deformation field monitoring at the centimeter level, or even millimeter-level deformation. The basic data processing flow of DInSAR is illustrated in the diagram below Figure 3:

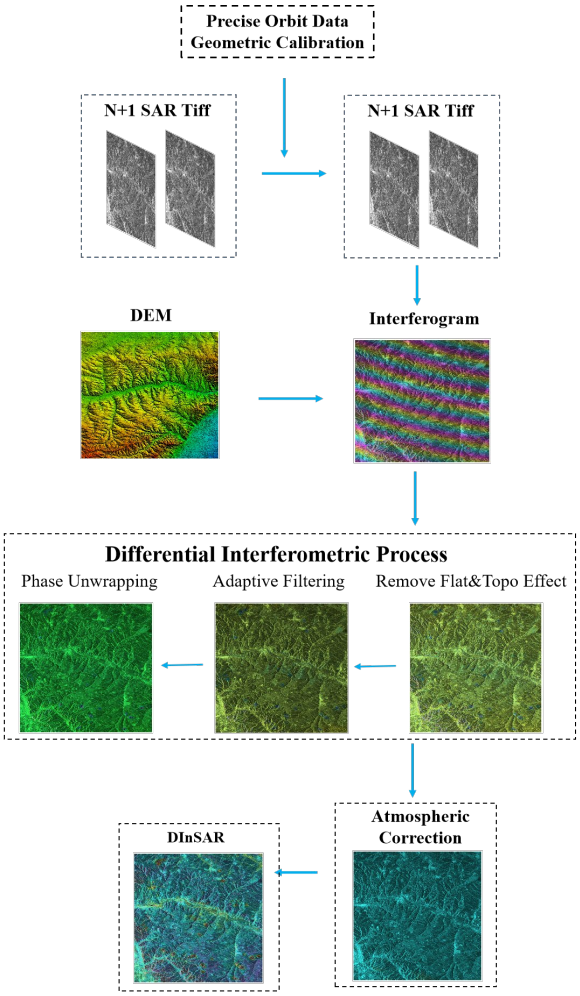

Figure 3. Flowchart of two-track DInSAR method

3. Study Area and Dataset

3.1 Study Area

The research area is located within Jinan City in Shandong Province, China. The Jinan to Zaozhuang high-speed railway mainline has a total length of 265.57 km, with a newly constructed mainline of 260.32 km and utilizing 5.25 km of existing infrastructure. The designed operating speed is 350 km per hour. The total length of newly constructed mainline bridges and tunnels is 214.222 km, accounting for 81.3% of the total railway length. Among these, the bridge length is 178.027 km, representing 67.6% of the total length, and the tunnel length is 36.195 km, constituting 13.7% of the total length(Ge, K., Wang, Y., Yu, C., et al, 2017). Additionally, there is a newly constructed Jinan East-Jiaozhou Yard connecting line of 6.812 single-track kilometers and a Jilai-Jibin connecting line of 6.097 single-track kilometers. The monitoring area is shown in Figure 4.

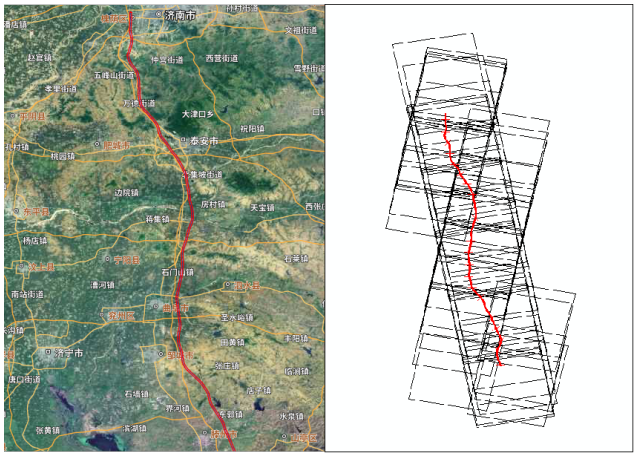

Figure 4. Monitoring Area and Image Coverage

3.2 Dataset

This article primarily utilizes SAR data processing software developed independently by the National Satellite Remote Sensing Application Center of the Ministry of Natural Resources(Ma, T., Tan, H., Li, T., et al. 2021), known as LandSAR. For the surface deformation measurement experiment along the railway in Jinan, Shandong, a total of 15 scenes of Lutan-1 SAR images covering the area were selected as the data source, and on-site measurements were conducted for validation (Zhang, T., Shi, Y., Wang, J., et al, 2021). Among these, 15 scenes of follow-mode data were used for deformation measurement (Cheng, P., Wen, H., Liu, H., et al, 2019), and the configuration parameters for the data are provided in Table 3, including a strip imaging mode, a resolution of 3 m, and a swath width of 50 km × 50 km.

Images	Shooting Satellite	Image	Shooting Satellite
20230701	LT-A	20230818	LT-A
20230623	LT-A	20230627	LT-B
20230911	LT-A	20230814	LT-B
20230611	LT-B	20230530	LT-A
20230619	LT-B	20230915	LT-B
20230705	LT-B	20230914	LT-A
20231009	LT-B	20230811	LT-B

Table 3. LuTan-1 SAR Satellite Data Acquisition Dates

4. Experiment and Results Analysis

4.1 Results Analysis

The surface deformation field product along the railway (Chen, D., Lu, Y., Jia, D, 2018)line in the Jinan to Zaozhuang region occurred from June 2023 to December 2023 . Among them, the descending data has a maximum vertical baseline of 206 m and a maximum temporal baseline of 80 days. This combination meets the requirements for high-precision observations. In the first phase of deformation product production, 15 scenes of L-SAR data were used, processing 28 interferometric pairs, obtaining 48 deformation field products, and completing the deformation field product for this region. The results are shown in the Figure 5.

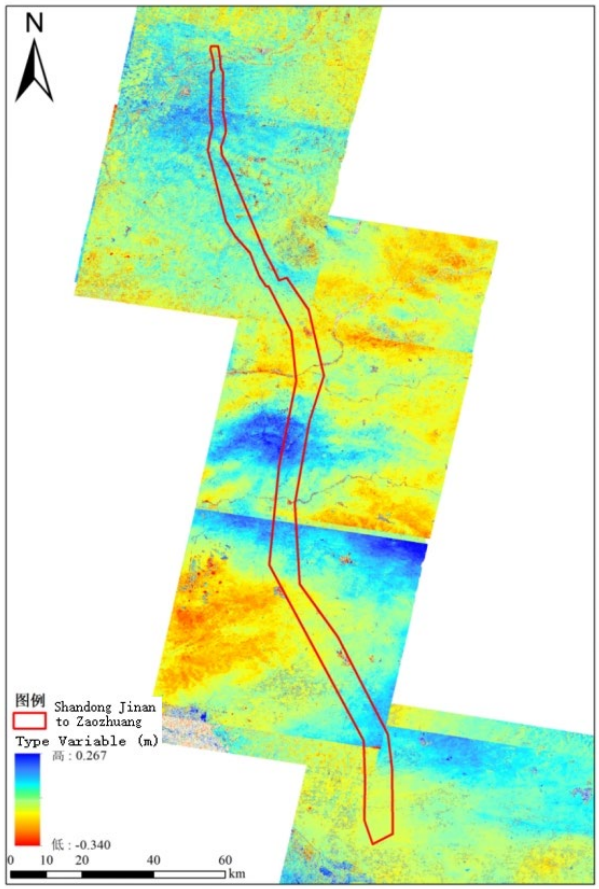

Figure 5. Deformation Monitoring Results

The monitoring results of the research area from July 5 to September 15, 2023, are shown in Figure 6. The railway section is located in mountainous terrain with various human activities, such as urban terraced fields. It can be observed that there are four suspected deformation hazards along the Jinan-Zaozhuang section, mainly related to slope stability. Due to the strong revisit capability and longer wavelength of the LuTan-1 satellite, with a 350 m baseline, significant subsidence along the railway line was detected using LuTan-1 SAR data. From July 5 to September 15, 2023, the maximum deformation amount (LOS direction) along the Jinan-Zaozhuang railway line reached 34 cm within a 48-day time interval.

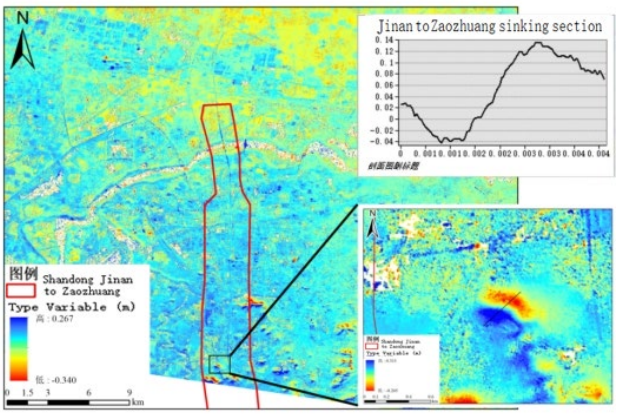

Figure 6. Deformation Monitoring Results from July to September

After calculating the deformation rate in Chengdu urban area using time-series InSAR technology, a buffer zone with a range

of 500 m was established along the Jinan-Zaozhuang railway line using vector data. This buffer zone was utilized to extract the deformation rate field along the Jinan-Zaozhuang railway line, and the extraction results are shown in Figure 7. It can be observed that within the time period from June 2023 to December 2023, the deformation rates along the 500 m buffer zone of the Jinan-Zaozhuang railway line range from -8 cm/year to 44 cm/year, indicating a region with relatively significant subsidence.

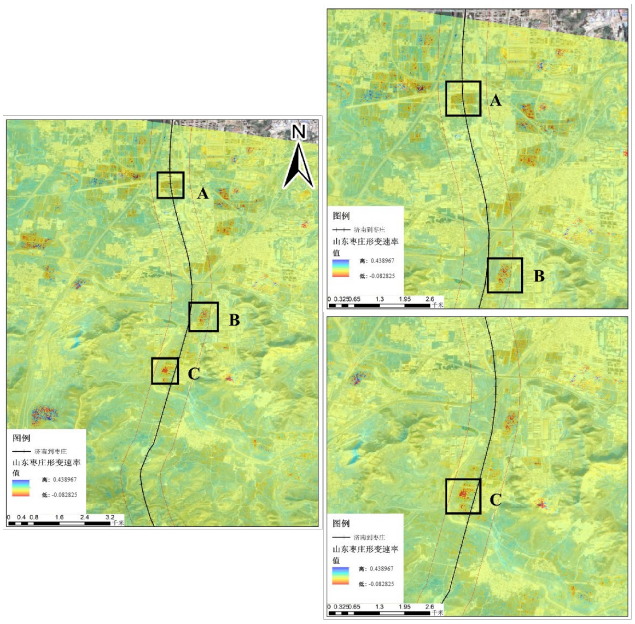

Figure 7. Stacking Strain Rate Products

4.2 Accuracy verification

To verify the accuracy of the DInSAR results during the study period and assess the reliability of ground deformation monitoring using LuTan-1 data, this experiment selected GPS data from 30 points in the Jinan area of Shandong for accuracy assessment, the distribution of some collected points is shown in the Figure 8. The surface deformation monitored by the DInSAR method is in the direction of the SAR satellite line of sight, whereas the deformation(Shi, G., Chen, Q., Liu, X., et al, 2022) observed by GPS includes both vertical and horizontal components. In order to accurately assess the precision of using LuTan-1 data with the DInSAR method, it is necessary to convert the horizontal movement and vertical deformation of the ground observation station into the SAR satellite line of sight. The transformation formula is as follows:

$$D_{los} = \cos\theta \bullet D_v - \sin\theta \bullet \cos\beta \bullet D_e + \sin\theta \bullet \sin\beta \bullet D_n \qquad (9)$$

In the formula, D_{los} represents the deformation in the satellite line of sight; D_v represents the vertical subsidence; D_e represents the deformation in the east-west direction; D_n represents the deformation in the north-south direction; θ represents the radar incidence angle; β represents the azimuth angle of the satellite.

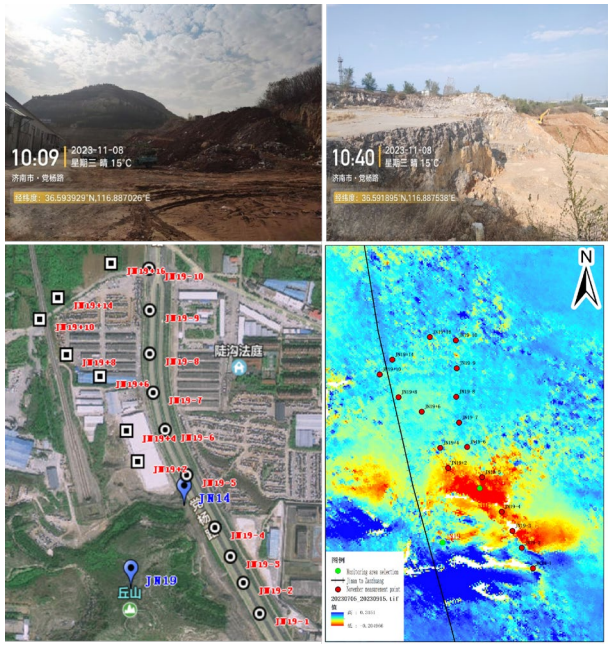

Figure 8 Distribution of GPS measurement points

Statistical analysis of the GPS and DInSAR results for corresponding points is shown in Figure 9. Based on the measured GPS data, it was found that the deformation trends of the GPS and DInSAR results for corresponding points were generally consistent(Yao, W., Xu, K., Zhu, X., et al. 2021). However, there were some discrepancies in individual point values, which could be attributed to factors such as personnel and equipment, leading to relatively lower measurement accuracy. Further efforts will be made to improve the measurement precision through multiple or high-precision field measurements to obtain more accurate detection results. The statistical analysis indicates that the average absolute error of the DInSAR deformation results is 4.62 mm, and the root mean square error is 5.83 mm, meeting the design accuracy requirements.

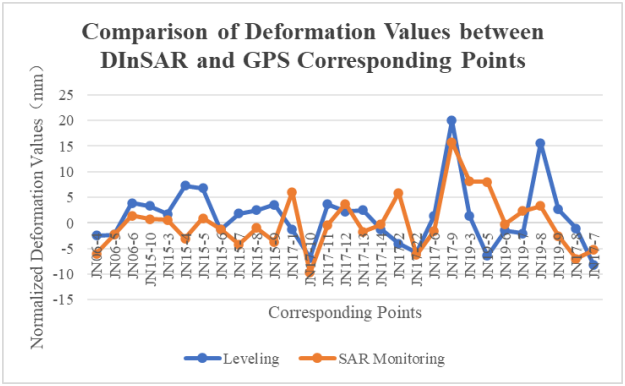

Figure 9. Comparison of Deformation Values between DInSAR and GPS Corresponding Points

5. Conlusions

The results indicate that the DInSAR results obtained using LuTan-1 SAR data are highly consistent with on-site measurement results, providing accurate monitoring outcomes for the research area. Compared to leveling measurements, LuTan-1 DInSAR deformation monitoring demonstrates a superior accuracy of 5 cm (RMSE). Stacking result can be

observed that Jinan-Zaozhuang railway line range from -8 cm/year to 44 cm/year, indicating a region with relatively significant subsidence.The quantitative results validate the effectiveness of LuTan-1 SAR data in railway deformation monitoring.Two comparisons show that InSAR monitoring technology has great potential for promotion in high-speed railway monitoring, making the use of InSAR monitoring methods a new choice for monitoring future railway settlement.

Acknowledgment

This research was supported by the National Natural Science Foundation of China (41901303), National Key R&D Programme of China (2021YFC3000405), Civil Spaceflight Pre-Research Projects (D010206) and autonomous research subject of land satellite remote sensing application key laboratory (BN2302-8).

References

High, W., (2020). Application of DInSAR Subsidence Monitoring Technology in Railway Area Subsidence Monitoring. Railway Survey, 46(06), 18-23+32.

Gao, W., Gan, J., & Wang, C. (2015). Application of DInSAR Subsidence Monitoring Technology in Railway Survey and Design. Remote Sensing Information, 30(05), 83-87.

Li, H. (2015). Application of InSAR Technology in Ground Subsidence Monitoring. Electronic Technology and Software Engineering, (22), 96-97.

Zhang, T., Shi, Y., Wang, J., et al. (2021). Analysis of Subsidence Prediction Model with InSAR and Improved Support Vector Machine. Surveying Science, 46(11), 63-70.

Cheng, P., Wen, H., Liu, H., et al. (2019). Current Status and Development Trends of Satellite Geodesy. Journal of Wuhan University (Information Science Edition), 44(01), 48-54.

Wang, Z., Xu, S., Wang, N., et al. (2018). Application of High-Resolution Optical and SAR Remote Sensing Images in Seismic Geological Hazard Investigation—A Case Study of the M7.0 Earthquake in Jiuzhaigou. Journal of Geological Hazards and Prevention, 29(05), 81-88.

Ji, Z., Bo, H., Wang, D., et al. (2019). "Monitoring and Analysis of Coal Mining Subsidence in Jining City Based on DInSAR." Shandong Land and Resources, 35(02), 38-43.

Ge, K., Wang, Y., Yu, C., et al. (2017). Establishment of Environmental Protection Evaluation System for Railway Construction Projects—A Case Study of the Lhasa to Nyingchi Section of the Newly-built Sichuan-Tibet Railway. Environmental Protection, 45(17), 60-64.

Ma, T., Tan, H., Li, T., et al. (2021). "Road Extraction from High-Resolution Satellite Imagery using Dilated Convolution Residual Networks with Multi-scale Feature Fusion." Progress in Laser and Optoelectronics, 58(02), 341-348.

Chen, D., Lu, Y., Jia, D. (2018). Surface Deformation Monitoring in Changzhou Area Based on StaMPS-InSAR. Yangtze River, 49(12), 59-65.

Shi, G., Chen, Q., Liu, X., et al. (2022). "Monitoring Along-Slope Deformation Velocity Field of Taoping Township Ancient Landslide Using Joint Ascending and Descending Orbit Sentinel-1A Data." Journal of Engineering Geology, 30(04), 1350-1361. DOI: 10.13544/j.cnki.jeg.2020-016.

Yao, W., Xu, K., Zhu, X., et al. (2021). "Crustal Deformation Characteristics and Mechanisms Following the 2015 Nepal MW7.8 Earthquake: A GNSS Observational Study." Journal of Geodesy and Geodynamics, 41(08), 833-840. DOI: 10.14075/j.jgg.2021.08.012.